

## DESIGN OF A TWO-ELEMENT AIRFOIL IN A RANGE OF ANGLES OF ATTACK

D. F. Abzalilov

UDC 532.5.031-2:533.6.011.32:533.694.2

A numerical-analytical solution of an inverse boundary-value problem of aerohydrodynamics is obtained for a two-element airfoil in the full formulation, based on the velocity distribution defined on the sought airfoil contours in a range of angles of attack. It is demonstrated that flow separation does not occur in the entire range considered for a specified non-separated velocity distribution on the upper surfaces at the maximum angle of attack and on the lower surface at the minimum angle of attack. An example of constructing a sectional airfoil is given; verification of the results obtained is performed with the use of the Fluent software package.

**Key words:** inverse boundary-value problems, airfoil, range of angles of attack.

Design of multi-element airfoils with optimal aerodynamic characteristics is an urgent problem [1, 2]. The approach used in [1, 2] implies airfoil modification by the method of adjoint gradients. The calculations are performed on multiprocessor supercomputers by multiple solutions of the problem of a viscous flow around a multi-element airfoil. Such a problem, however, can also be solved on a usual personal computer by applying the theory of inverse boundary-value problems of aerohydrodynamics [3].

Abzalilov et al. [4] solved the problem of design of a two-element airfoil in an ideal incompressible fluid flow, based on the velocity or pressure distribution specified on the airfoil surface. From the practical viewpoint, it seems of interest to design airfoils with specified aerodynamic characteristics for a certain range of angles of attack rather than for one angle of attack. Let us consider the problem solved in [4], with the only difference that the initial data of the problem, namely, the velocity distributions, are specified for two different angles of attack.

The problem is solved in the following formulation. In a physical plane  $z$  (Fig. 1a), the sought two-element airfoil  $A_kB_k$  ( $k = 1, 2$ ) is exposed to a steady irrotational flow of an ideal incompressible fluid at two angles of attack ( $\alpha$  and  $\alpha^*$ ); the difference  $\delta = \alpha^* - \alpha > 0$  is assumed to be given. The airfoil contours  $L_{zk}$  are assumed to be smooth, except for the trailing edges  $B_k$ , where the internal (with respect to the flow domain) angles are  $2\pi$ .

The origin of the Cartesian coordinate system is chosen on the trailing edge  $B_1$  of the contour  $L_{z1}$ , and the abscissa axis is parallel to the direction of the specified free-stream velocity vector  $v_\infty$ . The contour perimeters are known and equal to  $l_k$ . The arc abscissas  $s_k$  of the airfoil contours are counted from zero at the points of  $B_k$  to  $l_k$  at the same points, so that the flow domain remains on the left with increasing  $s_k$ . Each contour is divided into two parts (upper and lower surfaces) by the point  $C_k$  ( $s = s_{ck}$ ). The velocity distributions on the airfoil contour  $L_{zk}$  are specified for the angle of attack  $\alpha$  on the lower surface and for the angle of attack  $\alpha^*$  on the upper surface:

$$v = \begin{cases} v_k(s_k), & s_k \in [0, s_{ck}], \\ v_k^*(s_k), & s_k \in [s_{ck}, l_k], \end{cases} \quad k = 1, 2. \quad (1)$$

An example of such a parametric distribution of velocities  $v_k(s_k)$  and  $v_k^*(s_k)$  is given in Fig. 2.

The contour positions are fixed by setting the difference between the complex potentials at the points  $A_2$  and  $A_1$  at the angle of attack  $\alpha$ :  $w(z_{a2}) - w(z_{a1}) = \varphi_{a2} + i\psi_{a2}$ .

---

Chebotarev Institute of Mathematics and Mechanics, Kazan' State University, Kazan' 420008; damir.abzalilov@ksu.ru. Translated from Prikladnaya Mekhanika i Tekhnicheskaya Fizika, Vol. 49, No. 6, pp. 107–114, November–December, 2008. Original article submitted November 7, 2007.

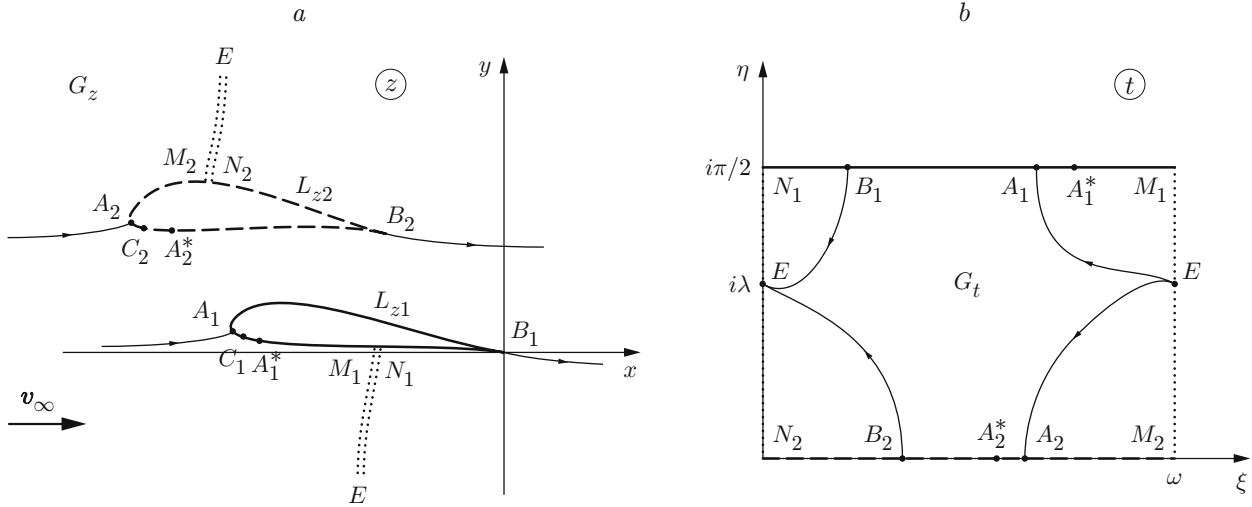


Fig. 1. Flow domain in the physical (a) and canonical (b) planes.

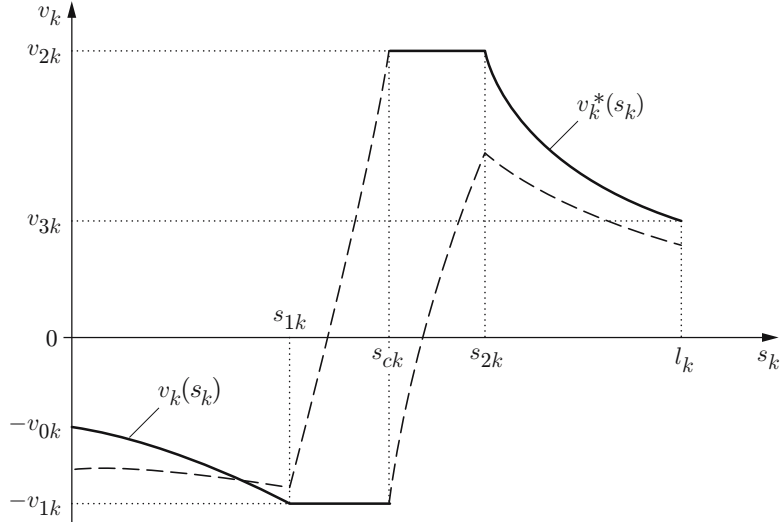


Fig. 2. Parametric distribution of velocity for solving the problem in the range of angles  $[\alpha, \alpha^*]$ : the solid and dashed curves show the specified distribution and the distribution obtained after solving the problem, respectively.

We reduce the problem posed to a problem for one angle of attack by recalculating the distributions  $v_k^*(s_k)$  for the angle  $\alpha$ .

We find a conformal mapping of the doubly connected domain  $G_z$  in the plane  $z$  onto a rectangle  $G_t$  with sides  $\omega_1 = \omega$  and  $\omega_2 = i\pi/2$  in the plane  $t = \xi + i\eta$ . The side  $N_1 M_1$  of the rectangle  $G_t$  in the plane  $t$  corresponds to the contour  $L_{z1}$ , the side  $N_2 M_2$  corresponds to the contour  $L_{z2}$  (Fig. 1b), an infinitely distant point in the plane  $z$  transforms to the point  $E$  ( $t = i\lambda$ ) on the imaginary axis, and the condition of periodicity is satisfied on the lateral sides of the triangle.

According to the solution of a direct problem on a biplane [5], we can write expressions for the complex potential  $w(t)$  and complex-conjugate velocity  $u(t)$  of the flow in the rectangle:

$$w(t) = \varphi(\xi, \eta) + i\psi(\xi, \eta) = u_\infty [e^{i\beta} \zeta(t - i\lambda) + e^{-i\beta} \zeta(t + i\lambda)] + \frac{\Gamma_1 + \Gamma_2}{2\pi i} \ln \frac{\sigma(t - i\lambda)}{\sigma(t + i\lambda)} + Kt + C; \quad (2)$$

$$u(t) \equiv \frac{dw}{dt}(t) = -u_\infty [e^{i\beta} \rho(t - i\lambda) + e^{-i\beta} \rho(t + i\lambda)] + \frac{\Gamma_1 + \Gamma_2}{2\pi i} [\zeta(t - i\lambda) - \zeta(t + i\lambda)] + K. \quad (3)$$

Here

$$K = (-\Gamma_1 + (\Gamma_1 + \Gamma_2)\lambda\eta_1/\pi - 2u_\infty\eta_1\cos\beta)/\omega = \text{const},$$

$u_\infty$  and  $\beta$  are the power and moment of the dipole at the point  $E$ ,  $C = C_1 + iC_2$  is a complex constant,  $\rho(t)$ ,  $\zeta(t)$ , and  $\sigma(t)$  are the Weierstrass functions with half-periods  $\omega/2$  and  $i\pi/2$ , and  $\eta_1 = \zeta(t+\omega) - \zeta(t)$  is a constant depending on  $\omega$ .

Note that a change in the angle of attack implies the relation

$$z(t) = z^*(t)e^{i\delta}, \quad (4)$$

which yields the dependence

$$v_k(\xi) = v_k^*(\xi) \frac{u_k(\xi)}{u_k^*(\xi)} \quad (5)$$

[ $u_1(\xi) \equiv u(\xi + i\pi/2)$ ,  $u_2(\xi) \equiv u(\xi)$ , and the function  $u(t)$  is determined by Eq. (3)]. As the distributions of  $v_k(s_k)$  rather than  $v_k(\xi)$  are specified, Eq. (5) cannot be used for recalculating  $v_k^*(s_k)$  for the angle  $\alpha$  without finding the dependence  $s_k(\xi)$ .

The function  $u(t)$  is determined by six unknown parameters:  $\omega$ ,  $\lambda$ ,  $u_\infty$ ,  $\beta$ ,  $\Gamma_1$ , and  $\Gamma_2$ . Instead of two last parameters, it seems reasonable to specify  $\xi_{b1}$  and  $\xi_{b2}$ , which are the positions of flow separation in the canonical plane, because they remain unchanged with variations of the angle of attack. For the angle  $\alpha^*$ , we obtain a new function  $u^*(t)$  depending on new parameters  $\omega^*$ ,  $\lambda^*$ ,  $u_\infty^*$ ,  $\beta^*$ ,  $\xi_{b1}^*$ , and  $\xi_{b2}^*$ . It follows from Eq. (4) that  $\omega^* = \omega$ ,  $\lambda^* = \lambda$ ,  $u_\infty^* = u_\infty$ ,  $\beta^* = \beta - \delta$ ,  $\xi_{b1}^* = \xi_{b1}$ , and  $\xi_{b2}^* = \xi_{b2}$ .

Thus, we determined all parameters for reconstructing the function  $u^*(t)$ . It follows from Eq. (5) that

$$\frac{v_k^{*\prime}(\xi)}{v_k^*(\xi)} - \frac{v_k'(\xi)}{v_k(\xi)} = U_k(\xi), \quad U_k(\xi) \equiv \frac{u_k^{*\prime}(\xi)}{u_k^*(\xi)} - \frac{u_k'(\xi)}{u_k(\xi)}.$$

Based on the form of the functions  $U_k(\xi)$ , we can see whether the ratio  $v'(s)/v(s)$  increases or decreases as the angle of attack is changed. As an example, we consider the upper surface of the first contour. This surface corresponds to the interval  $\xi \in [\xi_{b1}, \xi_{a1}^*]$ , where  $U_1(\xi) > 0$ . Hence,  $v_1^{*\prime}(\xi)/v_1^*(\xi) > v_1'(\xi)/v_1(\xi)$ . As the inequalities  $ds/d\xi < 0$ ,  $v_1^*(\xi) > 0$ , and  $v_1(\xi) > 0$  are satisfied on the interval considered, we obtain

$$\frac{v_1^{*\prime}(s)}{v_1^*(s)} < \frac{v_1'(s)}{v_1(s)}. \quad (6)$$

The distribution  $v_1^*(s)$  [see Eq. (1)] is set on the upper surface. As was shown in [6], if this distribution is non-separated, then any distribution  $v_1(s)$  satisfying Eq. (6) is also non-separated.

Studying all segments in this manner, we come to the following conclusion: if the velocity distributions specified on the lower surfaces for the angle of attack  $\alpha$  and on the upper surfaces for the angle of attack  $\alpha^*$  are non-separated, then the flow around a two-element airfoil is non-separated in the entire range  $[\alpha, \alpha^*]$ .

From the known distributions  $v_k(s_k)$  (1), we find the functions

$$\varphi_k(s_k) = \int_0^{s_k} v_k(\tilde{s}_k) d\tilde{s}_k, \quad s_k \in [0, s_{ck}], \quad \varphi_k^*(s_k) = \int_{s_k}^{l_k} v_k^*(\tilde{s}_k) d\tilde{s}_k, \quad s_k \in [s_{ck}, l_k]. \quad (7)$$

Let us introduce the following notations:

$$\Phi_k \equiv \varphi_k(s_{ck}) = \int_0^{s_{ck}} v_k(\tilde{s}_k) d\tilde{s}_k, \quad \Phi_k^* \equiv \varphi_k^*(s_{ck}) = \int_{s_{ck}}^{l_k} v_k^*(\tilde{s}_k) d\tilde{s}_k.$$

The functions  $w(t)$  and  $w^*(t)$  are determined from Eq. (2). Let  $\xi_{ck}$  be the real parts of the positions of the points  $C_k$  in the plane  $t$ . We consider the functions

$$\begin{aligned} \varphi_1(\xi) &= w(\xi + i\pi/2) - w(\xi_{b1} + \omega + i\pi/2), & \xi \in [\xi_{c1}, \xi_{b1} + \omega], \\ \varphi_2(\xi) &= w(\xi) - w(\xi_{b2}), & \xi \in [\xi_{b2}, \xi_{c2}], \\ \varphi_1^*(\xi) &= w^*(\xi_{b1} + i\pi/2) - w^*(\xi + i\pi/2), & \xi \in [\xi_{b1}, \xi_{c1}], \\ \varphi_2^*(\xi) &= w^*(\xi_{b2} + \omega) - w^*(\xi), & \xi \in [\xi_{c2}, \xi_{b2} + \omega]. \end{aligned} \quad (8)$$

By comparing the complex potentials in the physical and canonical planes, we obtain the relations

$$\varphi_1(\xi_{c1}) = \Phi_1, \quad \varphi(\xi_{c2}) = \Phi_2, \quad \varphi^*(\xi_{c1}) = \Phi_1^*, \quad \varphi^*(\xi_{c2}) = \Phi_2^*. \quad (9)$$

By comparing functions (7) and (8), we find functions  $s_k(\xi)$  independent of the angle of attack.

Let us find the dependences  $v_k(\xi) = v_k[s_k(\xi)]$  and  $v_k^*(\xi) = v_k^*[s_k(\xi)]$ . Recalculating the distributions  $v_k^*(\xi)$  over the mapping of the upper boundary of the canonical domain for the angle  $\alpha$  by Eq. (5), we obtain the distributions  $v_k(\xi)$  over the entire interval  $\xi \in [0, \omega]$ .

To solve the further problem, we use the method of solving an inverse problem for one angle of attack [4]. We consider a modified Joukowski–Mitchell function  $\chi(t)$  in the form

$$\chi(t) = \ln \left( \frac{1}{v_\infty} \frac{dw}{dz} \right) - \chi_0(t), \quad \chi_0(t) = \ln \left( \sin \frac{\pi(t - t_{a1})}{\omega} \sin \frac{\pi(t - t_{a2})}{\omega} \right).$$

The function  $\chi(t) = S(\xi, \eta) + iT(\xi, \eta)$  is periodic and has no singularities in the entire rectangle  $G_t$ . The real part of this function on the upper and lower sides of the rectangle  $G_t$  is known:

$$S_1(\xi) = \ln \left| \frac{v_1(s_1(\xi))}{v_\infty} \right| - \ln \left| \sin \frac{\pi(\xi - \xi_{a1})}{\omega} \sin \frac{\pi(\xi - \xi_{a2} + i\pi/2)}{\omega} \right|,$$

$$S_2(\xi) = \ln \left| \frac{v_2(s_2(\xi))}{v_\infty} \right| - \ln \left| \sin \frac{\pi(\xi - \xi_{a2})}{\omega} \sin \frac{\pi(\xi - \xi_{a1} - i\pi/2)}{\omega} \right|.$$

Here  $S_1(\xi) = S(\xi, \pi/2)$  and  $S_2(\xi) = S(\xi, 0)$ .

The function  $\chi$  can be reconstructed by Ville's formula (see, e.g., [7])

$$\chi(t) = \frac{1}{i\pi} \int_0^\omega \left[ S_1(\xi) \zeta \left( t - \xi - \frac{i\pi}{2} \right) - S_2(\xi) \zeta(t - \xi) \right] d\xi + \frac{\eta_1 - 2}{2\omega} P_1 + iP_2,$$

where  $P_2$  is an arbitrary real constant; the quantity  $P_1$  is determined by the formula

$$P_1 = \int_0^\omega S_1(\xi) d\xi = \int_0^\omega S_2(\xi) d\xi. \quad (10)$$

Condition (10) is a condition of single-valuedness of the function  $\chi(t)$ .

Based on the known function  $\chi(t)$ , we find its imaginary part on the upper and lower sides of the rectangle  $G_t$ :  $T_1(\xi) = \text{Im } \chi(\xi + i\pi/2)$  and  $T_2(\xi) = \text{Im } \chi(\xi)$ .

After integrating the expression  $dz/dt = (dw/dt)/(dw/dz)$  over the upper and lower sides of the rectangle  $G_t$ , we find a parametric expression for the contours

$$z_k(\xi) = z_{0k} + \int_{\xi_{bk}}^{\xi} \frac{u_k(\xi)}{v_k(\xi)} e^{i\theta_k(\xi)} d\xi, \quad k = 1, 2, \quad (11)$$

where  $\theta_1(\xi) = -T_1(\xi) - \text{Im } \chi_0(\xi + i\pi/2)$  and  $\theta_2(\xi) = -T_2(\xi) - \text{Im } \chi_0(\xi)$  are the slopes of the tangent lines to the contours.

For the problem to be solved, four conditions (9) have to be satisfied. Using Eq. (5), we can obtain four more conditions from the conditions of continuity of velocity distributions at the points  $B_k$  and  $C_k$ :

$$\frac{v_k^*(s_{ck})}{v_k(s_{ck})} = \frac{u_k^*(\xi_{ck})}{u_k(\xi_{ck})}, \quad \frac{v_k^*(l_k)}{v_k(0)} = \frac{[u_k^*(\xi_{bk})]'}{[u_k(\xi_{bk})]'}, \quad k = 1, 2. \quad (12)$$

The conditions of closedness follow from Eq. (11):

$$\int_0^\omega \frac{u_k(\xi)}{v_k(\xi)} e^{i\theta_k(\xi)} d\xi = 0, \quad k = 1, 2. \quad (13)$$

As these conditions are complex, they are equivalent to four real conditions.

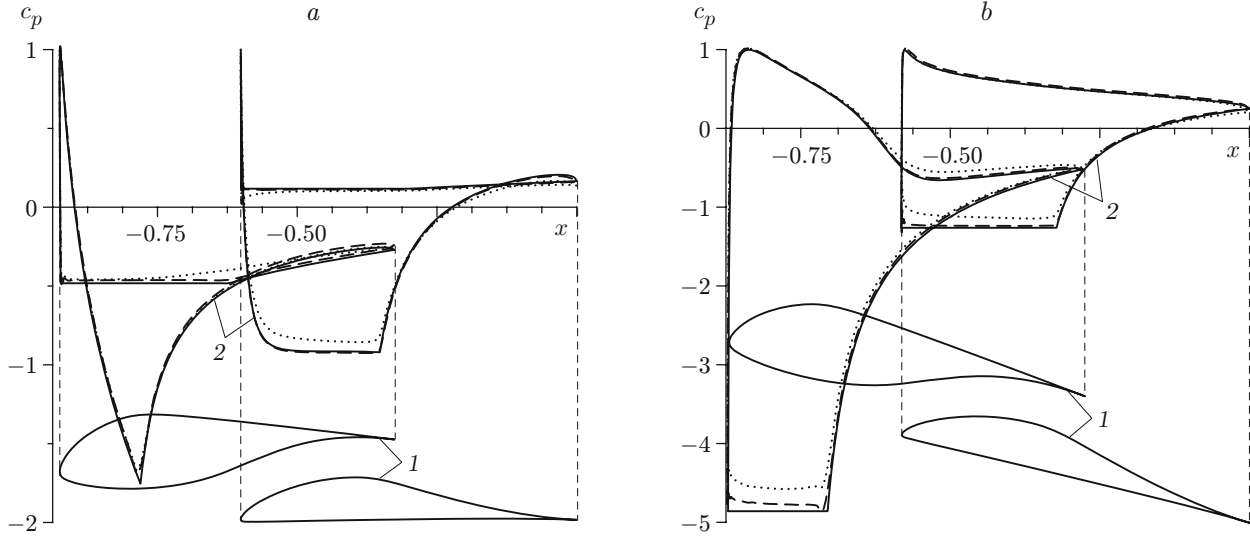


Fig. 3. Contours of a two-element airfoil (1) and distributions  $c_p(x)$  (2) for  $\alpha = 1^\circ$  (a) and  $\alpha^* = 2^\circ$  (b); the solid curves are the calculations by the IIF model, the dashed curves are the inviscid flow model, and the dotted curves are the calculations by the Spalart–Allmaras model of turbulent flow.

Taking into account the relation  $(dw/dz)\Big|_{z \rightarrow \infty} = v_\infty$ , we obtain  

$$\text{Im } \chi(i\lambda) = 0, \quad \text{Re } \chi(i\lambda) = 0. \quad (14)$$

The first equality in (14) serves to determine the unknown  $P_2$ , and the second equality is the condition of solvability. Another condition of solvability is the above-given condition (10). By adding two more conditions determining the functions  $\varphi_{a2}$  and  $\psi_{a2}$ , we obtain an extremely complicated problem with 16 restrictions.

The problem involves eight unknown parameters:  $\omega$ ,  $\lambda$ ,  $u_\infty$ ,  $\beta$ ,  $\xi_{b1}$ ,  $\xi_{b2}$ ,  $\xi_{c1}$ , and  $\xi_{c2}$ . As the number of parameters is smaller than the number of solvability conditions, the problem is solved either by using the method of quasi-solutions [3] or by introducing free parameters into the specified distributions  $v_k(s_k)$  and  $v_k^*(s_k)$ . Figure 2 shows the velocity distributions  $v_k(s_k)$  and  $v_k^*(s_k)$  in a parametric form, each of them being dependent on seven parameters  $v_{0k}$ ,  $v_{1k}$ ,  $v_{2k}$ ,  $v_{3k}$ ,  $s_{1k}$ ,  $s_{ck}$ , and  $s_{2k}$ . Thus, the problem has 22 free parameters.

As it is difficult to find parameters to satisfy 16 nonlinear conditions of solvability, the problem was solved in a semi-inverse formulation. The parameters  $\omega$ ,  $\lambda$ ,  $u_\infty$ , and  $\beta$  in the canonical plane were specified, and the airfoil perimeters  $l_k$  and the positions  $s_{ck}$  of the points  $C_k$  in the physical plane were to be found. The parameters  $\xi_{bk}$  rather than the values of  $\varphi_{a2}$  and  $\psi_{a2}$  were set to fix the positions of the airfoils. As a result, the sequence of the problem solution acquired the following form.

1. The parameters  $\delta$ ,  $\omega$ ,  $\lambda$ ,  $u_\infty$ ,  $\beta$ , and also  $\xi_{bk}$ ,  $s_{1k}$ , and  $s_{2k}$  ( $k = 1, 2$ ) are specified.
2. Conditions (9) are used to find  $s_{ck}$  and  $l_k$ .
3. Equations (12) are used to find  $v_{0k}$  and  $v_{1k}$ .
4. Satisfaction of the solvability conditions (10), (13), and (14) is ensured by choosing appropriate parameters  $\xi_{ck}$ ,  $v_{2k}$ , and  $v_{3k}$ .

Based on this sequence, a code for constructing a two-element airfoil was developed.

Figure 3 shows an example of airfoil construction in a range of angles of attack. The parameters  $\omega$ ,  $\lambda$ ,  $\beta$ , and  $\xi_{bk}$  are taken from the solution of the problem for one angle of attack [4]; the quantity  $u_\infty$  was found from the condition  $l_1 + l_2 = 1$ ; the range of the angles was  $\delta = 15^\circ$ . The characteristics of this airfoil are summarized in Table 1.

To verify the construction results, we calculated the flow around the constructed airfoil, using the Fluent software package. The computational grid (Fig. 4) was generated as follows: a circumference was described around the two-element airfoil, and a regular quadrangle grid was chosen outside of this circumference. An irregular triangular grid was used inside the circumference (except for the boundary layer, where a quadrangle grid was also used). A necessary angle of attack was achieved by turning the circumference.

TABLE 1

Characteristics of Two-Element Airfoils in a Range of Angles of Attack

$k$	$l_k$	$s_{ck}$	$v_{1k}$	$v_{2k}$	$\alpha$ , deg	$\alpha^*$ , deg	$c_y$	$c_y^*$
1	0.49	0.24	1.50	2.42	5.3	20.3	0.32	1.69
2	0.51	0.25	0.95	1.22				

TABLE 2

Aerodynamic Characteristics of Airfoils

Flow model	$c_{x1}$	$c_{y1}$	$c_{x2}$	$c_{y2}$
IIF model	0	0.32	0	1.69
Inviscid flow model	0.0011	0.31	0.0086	1.61
Spalart–Allmaras model of turbulent flow	0.0109	0.31	0.0277	1.55

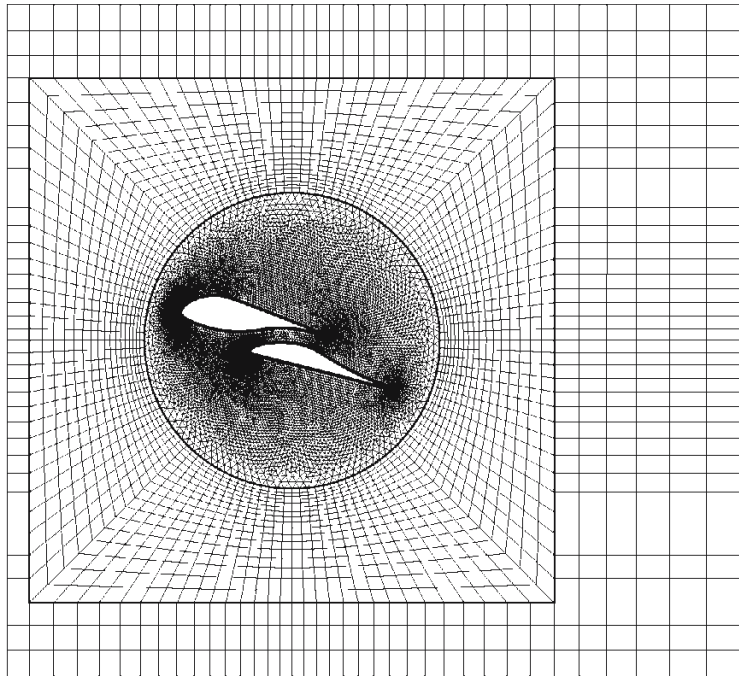


Fig. 4. Computational grid near the airfoil contour.

The following boundary conditions were imposed: the flow velocity on the input boundary of the computational domain, the exit condition on the exit boundary, the condition of symmetry or a smooth wall (with the velocity vector being parallel to the lateral boundary of the computational domain) on the lateral sides, and the no-slip condition on the airfoil surfaces.

The calculations were performed for two models: the inviscid flow model was used to verify the results of the numerical-analytical solution (model of an ideal incompressible fluid) and the Spalart–Allmaras model of turbulent flow was used to verify the applicability of the model of an ideal incompressible fluid (IIF) used to describe viscous flows ( $Re = 6 \cdot 10^6$ ).

The values of aerodynamic forces obtained by different models are listed in Table 2. It should be noted that the results of the exact numerical-analytical solution (IIF model) are in good agreement with the results calculated by the inviscid flow model. Some difference between the exact solution from the solution for turbulent flow is observed in the region between two contours, where viscous effects should be taken into account.

The author is grateful to N. B. Il'inskii for useful comments.

This work was supported by the Russian Foundation for Basic Research (Grant No. 05-08-01153).

## REFERENCES

1. T. Slawig, “Domain optimization of a multi-element airfoil using automatic differentiation,” *Adv. Eng. Software*, **32**, No. 3, 225–237 (2000).
2. S. Kim, J. J. Alonso, and A. Jameson, “Design optimization of high-lift configurations using a viscous continuous adjoint method,” AIAA Paper No. 2002-0844 (2002).
3. A. M. Elizarov, N. B. Il'inskii, and A. V. Potashev, *Inverse Boundary-Value Problems of Aerohydrodynamics: Theory and Methods of Design and Optimization of the Airfoil Shape* [in Russian], Fizmatlit, Moscow (1994).
4. D. F. Abzalilov, P. A. Volkov, and N. B. Il'inskii, “Solving an inverse boundary-value problem of aerohydrodynamics for a two-element airfoil,” *Izv. Ross. Akad. Nauk, Mekh. Zhidk. Gaza*, No. 3, 16–24 (2004).
5. L. I. Sedov, *Two-Dimensional Problems of Hydrodynamics and Aerodynamics* [in Russian], Nauka, Moscow (1966).
6. A. M. Elizarov and D. A. Fokin, “Design of airfoils providing a non-separated flow in a given range of variation of angles of attack,” *Iav. Akad. Nauk SSSR, Mekh. Zhidk. Gaza*, No. 3, 157–164 (1990).
7. N. I. Akhiezer, *Elements of the Theory of Elliptic Functions* [in Russian], Nauka, Moscow (1970).